

A computer screening approach to immunoglobulin superfamily structures and interactions: Discovery of small non-peptidic CD4 inhibitors as novel immunotherapeutics

(protein interactions/drug design/molecular data base/autoimmune diseases/organ transplantation)

SONG LI, JIMIN GAO, TAKASHI SATOH, THEA M. FRIEDMAN, ANDREA E. EDLING, UTE KOCH, SWATI CHOKSI, XIAOBING HAN, ROBERT KORNGOLD, AND ZIWEI HUANG*

Kimmel Cancer Institute, Jefferson Medical College, Thomas Jefferson University, Philadelphia, PA 19107

Communicated by Carlo M. Croce, Thomas Jefferson University, Philadelphia, PA, October 29, 1996 (received for review October 14, 1996)

ABSTRACT The interaction between CD4 and major histocompatibility complex (MHC) class II proteins is critical for the activation of CD4⁺ T cells, which are involved in transplantation reactions and a number of autoimmune diseases. In this study we have identified a CD4 surface pocket as a functional epitope implicated in CD4–MHC class II interaction and T-cell activation. A computer-based strategy has been used to screen ≈150,000 non-peptidic organic compounds in a molecular data base and to identify a group of compounds as ligands of the proposed CD4 surface pocket. These small organic compounds have been shown to specifically block stable CD4–MHC class II binding, and exhibit significant inhibition of immune responses in animal models of autoimmune disease and allograft transplant rejection, suggesting their potential as novel immunosuppressants. This structure-based computer screening approach may have general implications for studying many immunoglobulin-like structures and interactions that share similar structural features. Furthermore, the results from this study have demonstrated that the rational design of small non-peptidic inhibitors of large protein–protein interfaces may indeed be an achievable goal.

Protein–protein interactions are critical events in many biological processes. In general, these interactions involve large interfaces with many intermolecular contacts (1, 2). As such, it has long been a great challenge to design small molecular inhibitors of these surfaces in either peptide or more preferably non-peptide form. Recently, it has been suggested that proteins may actually interact through small critical surface-binding epitopes, as in the cases of the human growth hormone- (3) and the erythropoietin-receptor complexes (4). These findings raise the intriguing possibility that inhibitors of these small binding epitopes may be sufficient for the effective blockade of large protein–protein interfaces. However, the general validity of this hypothesis and its implication for rational drug design remain to be tested and demonstrated in different biological systems. Undoubtedly, the development of a general approach to inhibit protein–protein interactions will have a tremendous impact on the understanding of the structural basis of these interactions and the design of new therapeutic strategies for many human diseases.

An important category of protein–protein interactions are those among the immunoglobulin (Ig) superfamily of molecules, which includes a large group of cell surface structures that are characterized by a conserved Ig-like folding (5). The members of the Ig superfamily mediate diverse biological

functions in immunity, particularly in cell surface recognition, and thus are attractive targets for drug design studies. In an attempt to better understand the structural basis of Ig superfamily interactions, we have focused on the interaction between the CD4 protein and the major histocompatibility complex (MHC) class II protein. CD4 is a glycoprotein expressed on the surface of helper T cells, and consists of four Ig-like extracellular domains (D1–D4) (6). CD4 functions as a co-receptor for stabilizing the T-cell receptor interaction with antigen, presented by the MHC class II molecule expressed on an antigen presenting cell. CD4 is also involved in the signal transduction pathway, which leads to the activation of a helper T cell (7). CD4 binds to non-polymorphic regions of the MHC class II β 2 domain (8, 9), an interaction of low affinity ($>10^{-4}$ M) (10). While the crystal structures for both the CD4 D1D2 fragment and the MHC class II molecule have been determined (11–13), the structure of the CD4–MHC class II complex remains obscure. Numerous mutation studies of the CD4 protein have been carried out to determine the regions of CD4 involved in the MHC class II binding, and it is generally believed that the interface involves many contact sites over a large surface area of both the D1 and D2 domains (12, 14–16).

New computer technologies may have important impact on the discovery of small molecular inhibitors targeting protein–protein interfaces. Computer-based strategies exploit the structural information of the target molecules and specialized computational methods to propose novel therapeutic agents. In contrast to traditional approaches of random screening, which require laborious and expensive testing of large libraries of organic compounds, computational programs, such as DOCK (17), provide an efficient automatic method to screen large data bases of compounds to identify a small group of lead candidates for actual biological testing, thus saving an enormous amount of both time and money. While many studies using this computerized screening strategy have been reported in the discovery of novel enzyme inhibitors for diseases such as AIDS and parasitic infections (17, 18), the use of this approach to design inhibitors of Ig-related protein–protein interactions remains a largely unexplored area with great potential.

In this study we have applied the computer screening approach to select small non-peptidic organic molecules that could specifically inhibit the interaction between CD4 and MHC class II proteins, and thereby block the activation of CD4⁺ T cells. CD4⁺ T cells are known to play a role in the pathogenesis of autoimmune diseases, such as multiple sclerosis and rheumatoid arthritis, as well as mediate transplan-

The publication costs of this article were defrayed in part by page charge payment. This article must therefore be hereby marked “advertisement” in accordance with 18 U.S.C. §1734 solely to indicate this fact.

Copyright © 1997 by THE NATIONAL ACADEMY OF SCIENCES OF THE USA
0027-8424/97/9473-6\$2.00/0
PNAS is available online at <http://www.pnas.org>.

Abbreviations: MHC, major histocompatibility complex; EAE, experimental allergic encephalomyelitis; DMSO, dimethyl sulfoxide.
*To whom reprint requests should be addressed. Tel.: 215-503-4564; Fax: 215-923-2117; e-mail: Z_Huang@lac.jci.tju.edu.

tation reactions directed to allogeneic MHC class II antigens. Small molecular inhibitors of CD4–MHC class II interactions could therefore be used as effective immunosuppressants for these undesired T-cell responses. Furthermore, we used the CD4–MHC class II interaction as a template system to investigate Ig-related protein interactions and their potential for drug design. Because many Ig superfamily members use common structural features for protein–protein interactions, this small molecule approach developed from the CD4–MHC class II system could be applied to other Ig superfamily molecules involved in many different biological functions.

MATERIALS AND METHODS

Animals. Female SJL/J H2^s, male C57BL6/J (B6) H2^b, and male MHC class II mutant B6.C-H2^{bm12} (bm12) mice were purchased from The Jackson Laboratory. All animals used were between 7 and 9 weeks of age.

Computer Screening. The high resolution x-ray structure of the human CD4 D1 domain (11) containing a surface-binding pocket was used as a receptor for ligand docking. DOCK3.5 is an automatic computerized method used to screen small molecule data bases for possible ligands that could bind to a given receptor (19). Briefly, DOCK3.5 defined the CD4 surface pocket with a set of overlapping spheres, the centers of which became the potential locations for ligand atoms. The binding of an organic ligand to the CD4 surface pocket was judged both by shape complementarity and by a simplified interaction energy (force field energy). The Available Chemicals Directory (ACD) (Molecular Design Limited, San Leandro, CA) was chosen as the small molecular data base to be screened for potential ligands because it included approximately 150,000 commercially available small organic compounds. The structures of the molecules were generated computationally by using a heuristic algorithm, CONCORD, developed by R. Pearlman at the University of Texas.

Following a modified procedure of Ring *et al.* (18), 1000 molecules with the best shape complementarity scores and 1000 with the best force field scores were selected from a DOCK3.5 screening. The resulting 2000 compounds were then visually screened 3 times independently in the context of the CD4 D1 surface-binding pocket using the molecular display software INSIGHT II (Biosym Technologies, San Diego). In the first visual screening, no compound was selected in an attempt to get acquainted with the ligand-receptor complex. In the second and third screening, an effort was made to choose a set of diverse compounds that possessed distinctive chemical structures, receptor binding modes, and electrostatic and shape complementarity. Ultimately, 41 compounds were chosen for testing in the CD4–MHC class II cell adhesion assay. Of these 41 compounds, 37 were from the shape list, 15 were from the force field list, and 11 appeared on both lists.

Cell Adhesion Assay. The inhibition of stable CD4–MHC class II binding by the compounds selected from computer screening studies was assessed in a standard cell adhesion assay that has been shown by several laboratories to accurately reflect this functional interaction (8, 16, 20). Following a modified procedure of Moebius *et al.* (20), 5×10^4 COS-7 cells per well of a 6-well plate were transfected with T4-pcDNA3 (Invitrogen) by DOSPER liposomal transfection (Boehringer Mannheim) according to the supplier's protocol for the reagent. Normally, 30–40% of these transiently transfected COS-7 cells expressed human CD4, as determined by immunofluorescence. Raji B cells, expressing MHC class II molecules, were added (10^7 cells) in 1 ml of RPMI medium, containing 10% fetal calf serum and 200 mM glutamine, to each well 48 hr after transfection and incubated with transfected COS-7 cells at 37°C for 1 hr, in the presence or absence of an organic compound at appropriate concentrations. Inhibition of rosette formation was determined by the number of rosettes obtained in the presence of the organic compounds relative to the number of rosettes in the positive control.

COS-7 cells transfected with pcDNA3 vector alone served as a negative control with no rosette formation. Other studies have shown that the enumeration of rosetting as performed here correlates well with quantitative cell binding assays employing radiolabeled Raji cells (20).

To confirm the specificity of inhibition of the organic compounds, the compounds that inhibited the stable CD4–MHC class II binding were also tested in a similar cell adhesion assay for CD8–MHC class I binding. For this assay, COS-7 cells were transfected with T8-pcDNA3 and were mixed with Raji cells, as above, since they also expressed MHC class I molecules.

Murine Experimental Allergic Encephalomyelitis (EAE). The lead organic compounds were tested for *in vivo* immunosuppressive activity in murine EAE, an animal model for multiple sclerosis. An acute form of EAE was induced in SJL mice by subcutaneous challenge with the proteolipid epitope (21) (100 μ g in 0.15 ml PBS emulsified in an equal volume of complete Freund's adjuvant) on days 0 and 7. Pertussis (Michigan Biological Products, Lansing, MI) was administered intravenously (i.v.) 30 min after antigen injection on day 7 (0.25 ml containing 5×10^9 inactivated organisms). Clinical symptoms of EAE were evaluated based on a 0–5 scale of ascending severity of symptoms, as described (22). The administration of the organic compounds involved a single i.v. injection of the compounds (50 μ g) in 0.25% dimethyl sulfoxide (DMSO) (the compounds were not soluble in water) on day 12 post-challenge. The control injection of 0.25% DMSO alone showed that it had no effect on EAE in mice.

Murine Skin Allograft Rejection. The lead organic compounds were also tested for inhibition of CD4⁺ T-cell-mediated skin allograft rejection using the MHC class II disparate model of B6 mice challenged with bm12 tail skin. Three hours prior to skin transplantation, a single i.v. injection of the compounds (50 μ g in 0.25% DMSO) was administered. Following a modified method of Bailey and Usama (23), donor tail skin grafts (0.25 cm \times 0.5 cm) were transplanted onto the ventral side of the tail of the recipient mouse, covered with a glass tube and held into position with short strips of adhesive tape for 2 days. The tubes were removed and the grafts monitored every other day until all allogeneic grafts were rejected. Grafts that were initially accepted exhibited hair growth and full pigmentation. Syngeneic grafts were also transplanted as negative controls for rejection. Median survival times were calculated and statistical comparisons were performed by fully factorial MANOVA Tukey Test analysis using SYSTAT 5.2 software.

RESULTS AND DISCUSSION

A CD4 Surface Pocket Implicated in Functional MHC Class II Binding. The identification of a surface pocket on the CD4 molecule suitable for the binding of small organic ligands was critical to the successful implementation of the computer screening strategy for developing effective inhibitors of stable CD4–MHC class II binding. An approach combining theoretical prediction with verification by synthetic peptide experiments was used to search for these surface sites, as described (24). Theoretical analyses using surface ligand-binding site searching algorithms of APROPOS (25) and DOCK (19) and solvent-accessible surface area calculations (26) were carried out for the CD4 D1 domain to propose interesting surface structural features that might be involved in potential protein–protein interactions. Other computational methods such as DELPHI (27) were also used to analyze the electrostatic properties of CD4 surface structures. These analyses led to the identification of a potential site that appeared to be suitable for intermolecular binding. As shown in Fig. 1*a*, this CD4 D1 surface site consisted of the GFCC'C' sheet (residues 26–46 and 80–97 of the human CD4 protein) bound by FG (which is

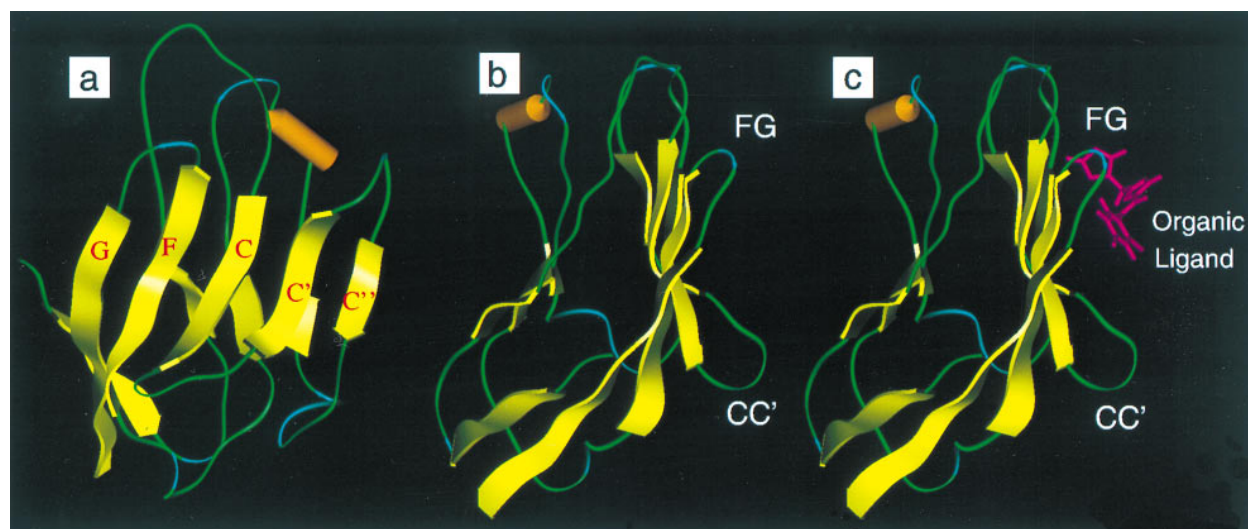


FIG. 1. A proposed surface-binding pocket on the CD4 D1 domain. (a) Front view of the pocket showing the potential involvement of the GFCC'C' sheet, and the FG, CC' and C'C' loops. (b) Side view of the pocket in *a* rotated 90°, highlighting the prominent role of the FG and CC' loops in forming this binding pocket. (c) CD4 surface pocket bound by an organic inhibitor TJU104 colored in cyan (see Fig. 2 for the chemical structure of TJU104).

also referred to as the third complementarity determining region or CDR3) (residues 86–89), CC' (residues 30–35) and C'C' (CDR2) (residues 40–43) loops. In particular, it was interesting to note that this site was walled in on either side by FG and CC' loops, which formed an intriguing surface pocket (Fig. 1*b*). Calculations of solvent accessible surface areas indicated that the FG and CC' loops were highly exposed. In addition, electrostatic potential calculations showed that the FG loop was part of a patch of negative electrostatic potential, whereas the CC' loop had a strong positive electrostatic potential (S.L. and Z.H., unpublished work). These results strongly supported the notion that the surface pocket played a prominent role in mediating molecular interactions.

The proposed CD4 D1 surface-binding pocket was consistent with available mutational data, which suggested that a large surface area of CD4 D1 is involved in MHC class II binding (12), and the FG (14) and C'C' (15, 16) loops have particularly been implicated in the interaction. The important role played by the FG loop in CD4 function has been suggested

by studies of synthetic peptides that mimic the site (28–31). Furthermore, a small cyclic heptapeptide mimicking the CC' loop has recently been shown to inhibit stable CD4–MHC class II interaction and CD4 mediated immune responses *in vitro* and *in vivo* (T. Satoh, J. M. Aramini, S.L., T. M. Friedman, J.G., A.E.E., R. Townsend, M. W. German, R.K., and Z.H., unpublished work).

Inhibitor Design Using a Computer Screening Approach.

The identification of a CD4 surface-binding pocket allowed the application of the computational screening approach to search $\approx 150,000$ non-peptidic organic compounds in the ACD data base for potential ligands of this pocket. This screening selected 41 compounds to be tested in the CD4–MHC class II cell adhesion assay. Eight of these compounds displayed significant inhibitory activity (range of 31–74%) in this assay at concentrations of 100 μM , with the structure of the four most potent organic inhibitors (TJU101–104) shown in Fig. 2. Further titration experiments indicated that these four organic compounds inhibited stable CD4–MHC class II interaction in

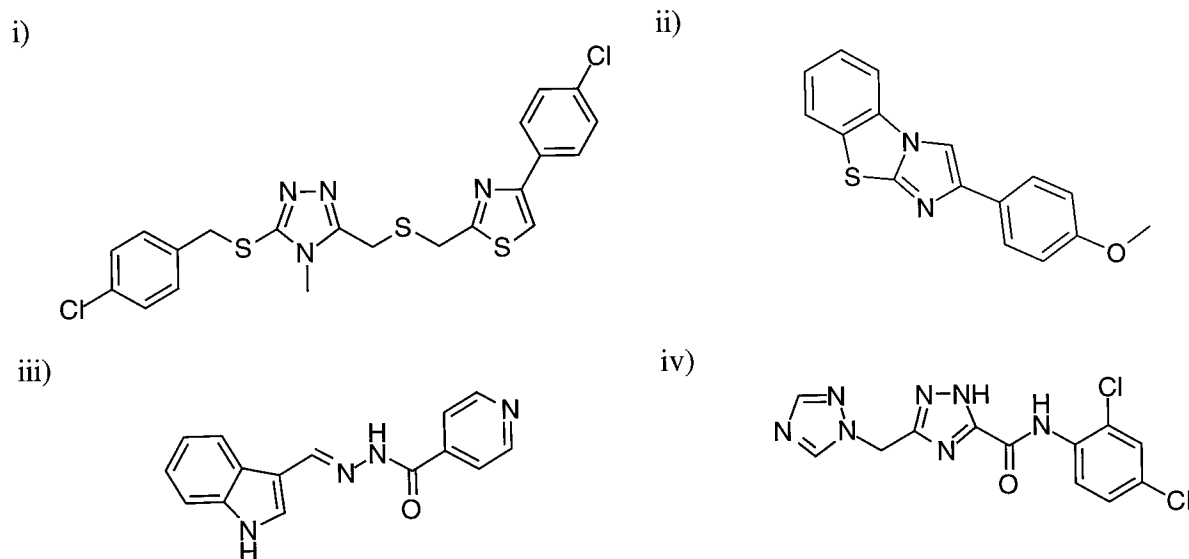


FIG. 2. Four non-peptidic organic inhibitors of stable CD4–MHC class II interactions: (i) TJU101, 5-(4-chloro-benzylthio)-3-[[4-(4-chlorophenyl)-2-thiazolyl]methylthiomethyl]-4-methyl-1,2,4-triazole; (ii) TJU102, 4-(4-methoxy-phenyl)-1-imidazo[2,1-B]benzothiazole; (iii) TJU103, *N*-(3-indolylmethylene)-isonicotinic hydrazine; (iv) TJU104, *N*-(2,4-dichloro-phenyl)-3-(1,2,4-triazol-1-ylmethyl)-1,2,4-triazole-5-carboxamide.

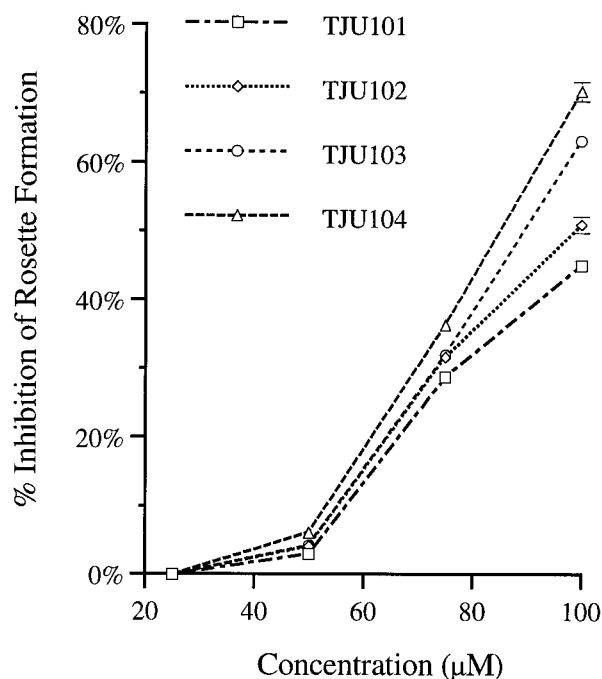


FIG. 3. Inhibitory activity by the four most potent organic compounds on CD4-MHC class II binding, as measured by the cell adhesion assay. The chemical structures of these compounds are given in Fig. 2. The points represent the mean of three independent assays.

a concentration dependent manner (Fig. 3), and this inhibition was specific, as demonstrated by their lack of activity in a CD8-MHC class I binding assay (data not shown). The structure of a representative organic inhibitor TJU104 docked into the CD4 surface pocket as proposed from computer docking calculations is shown in Fig. 1c.

Biological Activities of the Organic Inhibitors. The potent activity of the identified organic compounds in inhibiting stable CD4-MHC class II binding suggested that these compounds might block CD4⁺ T-cell activation. In this regard, the organic compounds (TJU101-104) were tested in human mixed lymphocyte reactions and were found to have inhibitory effects on alloreactive T-cell proliferation (data not shown). More importantly, *in vivo* studies were conducted to determine the immunosuppressive activity of these compounds in two animal models of CD4⁺ T-cell-mediated responses, involving autoimmunity and transplantation reactions. To ensure that the effect of the organic compounds *in vivo* was specific and not due to general cellular toxicity, we tested the four organic inhibitors (TJU101-104) for toxicity *in vitro* on mitogen-stimulated mouse T and B cells. Of these four compounds, TJU101 was found to exhibit non-specific toxicity (data not shown). The remaining three organic compounds (TJU102-104) were then tested *in vivo* and shown to have inhibitory activity on the development of EAE in SJL/J mice, in comparison with the untreated control group, when a single dosage (50 µg) was administered on day 12 after EAE induction (Fig. 4). TJU103 exhibited the most significant delay in the onset of disease and a decrease in the maximum mean severity score ($P < 0.05$ on day 16, the peak day of disease). These organic compounds were also assayed for activity in an MHC class II disparate skin allograft model (B6 mice challenged with bm12 tail skin grafts). All three compounds, when administered 3 hr prior to time of transplantation in a single dosage (50 µg *i.v.*), were found to prolong the median survival time of the allografts, in comparison to the untreated control mice (Fig. 5). TJU103 had the most significant effect among these organic compounds, extending survival to 52 days ($P \leq 0.002$). None of these three compounds exhibited any toxic effects *in vivo*,

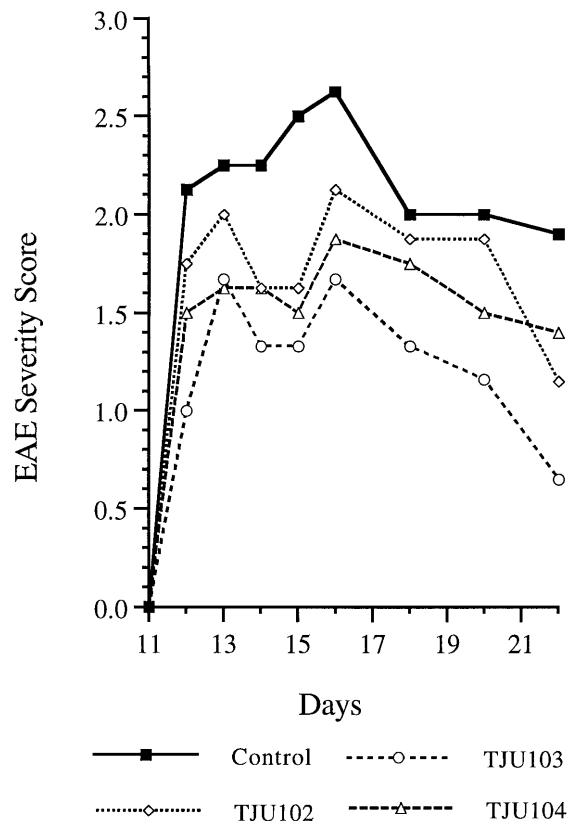


FIG. 4. Efficacy of the three selected organic compounds on the development of EAE severity in SJL/J mice. Mice were challenged subcutaneously (100 µg in 0.15 ml PBS emulsified in an equal volume of complete Freund's adjuvant) with the proteolipid epitope (p139-151) on days 0 and 7. Pertussis was administered 30 min after antigen injection on day 7 (0.25/ml containing 5×10^9 inactivated organisms, *i.v.*). The organic compounds were injected *i.v.* on day 12 at a dosage of 50 µg in 0.25 ml 0.25% DMSO. The mean severity score for each experimental group was calculated to include those mice that did not exhibit any symptoms of EAE. For all groups $n = 4$, except for TJU103 ($n = 3$).

with normal lymphocyte cellularity and subset composition in the spleen and lymph nodes of mice, 24 hr after injection (data not shown).

Therapeutic Potential of the Organic Inhibitors. The small non-peptidic organic inhibitors identified here may have important implications for the development of a new generation of non-toxic and orally available immunosuppressants for the treatment of autoimmune diseases and transplantation reactions. Current therapeutic strategies for these immunopathological conditions include the use of monoclonal antibodies (mAbs) such as anti-CD4 mAb (32) to block inflammatory T-cell activation. However, the inherent immunogenicity of xenogeneic mAbs have reduced their value as an effective treatment. In comparison with mAbs, small molecular inhibitors are likely to be less immunogenic. Also, in contrast to peptide-based therapeutics, non-peptidic organic structures are normally more stable and also more amenable for modifications using conventional medicinal chemistry and/or recent combinatorial chemistry techniques to improve potency and oral activity. For these reasons, the group of organic compounds with diverse and distinctive non-peptidic structures identified here may represent promising leads for the development of new immunosuppressive agents.

It should be pointed out that other strategies have been developed to convert biologically active peptides into analogs containing non-peptidic structural elements in the development of small molecular therapeutics. These strategies include

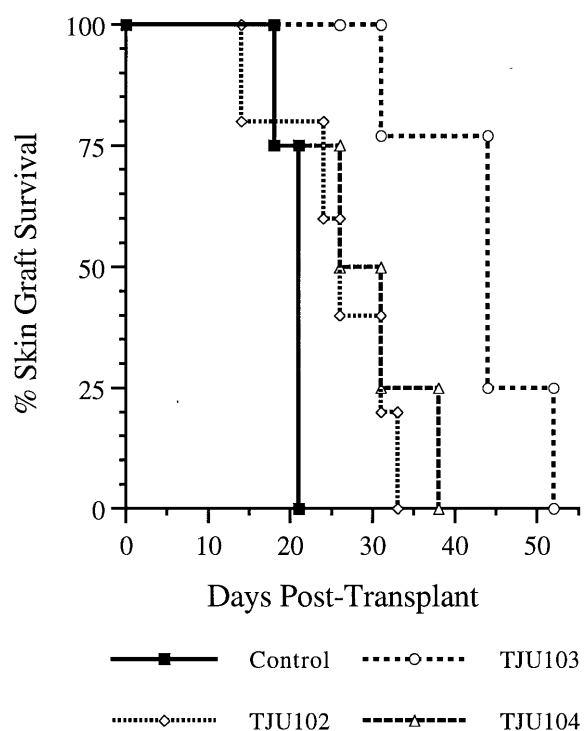


FIG. 5. Efficacy of the three selected organic compounds on allograft skin rejection. B6 mice were transplanted with either syngeneic or allogeneic (bm12) skin grafts. The compounds were injected 3 hr before transplantation at a dosage of 50 μ g in 0.2 ml 0.25% DMSO. For all groups $n = 4$, except for TJU102 ($n = 5$).

the peptidomimetic modification (33) and more recently the structure-based combinatorial chemistry techniques (34), which generally require extensive structure-activity studies of peptide ligands and subsequent synthetic modifications to incorporate non-peptide elements. The computer-based data base screening may represent an effective alternative approach to the discovery of non-peptidic leads. As shown in this study, the computer screening to generate non-peptidic ligands *de novo* was carried out based on the protein surface structure and required no prior knowledge about a peptide ligand. In addition, this process took less than a month of effort to select

41 possible lead candidates for biological testing. The success rate of identifying four potent compounds out of the selected 41 ($\approx 10\%$) in the cell adhesion assay is a significant improvement over the typical 0.01% yield from conventional random screening procedures (17).

Implications for Other Ig-Related Structures and Interactions. This study may provide a paradigm for the inhibitor design of many Ig-related protein structures and interactions. As members of the Ig superfamily have a conserved backbone folding pattern, it is likely that this generic structure provides some common scaffolds for efficient protein-protein interactions. In contrast to the view that CD4 uses its three CDR loops on the top for molecular interactions in a manner similar to the high-affinity antibody-antigen recognition (29, 31), we have proposed that the CC' loop, together with the FG (CDR3) loop, form a critical binding pocket on the lateral surface of CD4. It is interesting to note that similar surface pockets on other Ig-related proteins are also involved in molecular interactions and biological functions (Fig. 6). For example, a similar pocket consisting of the FG and CC' loops is commonly observed to be involved in dimerization of Ig superfamily molecules, such as homodimers of CD8 α (35) and antibody V_HV_L (40). On the other hand, this pocket also mediates heterophilic interactions as seen in Fc ϵ RI α_2 , which is the domain of the IgE high-affinity receptor that binds IgE (36), CD2 that binds LFA-3 (37), and CD28 that binds CD80/86 (38). It has been proposed that a common structural theme may mediate diverse homophilic and heterophilic interactions of Ig-related domains (41). The results of our study regarding the role of the CD4 surface pocket in mediating stable MHC class II interaction and T-cell activation are consistent with this notion. As these Ig-related proteins appear to use a similar surface pocket for their specific interactions and biological functions, it is possible that the computer screening approach developed from this study of the CD4 protein may also be applicable to the design of small non-peptidic inhibitors of other Ig superfamily molecular interactions.

Concluding Remarks. We have tested the hypothesis that non-peptidic organic inhibitors targeting a small functionally important surface epitope could be sufficient for the effective blockade of a protein-protein interaction with a large interface. Employing theoretical analysis of protein structure and subsequent synthetic peptide mapping approaches, we have identified a surface pocket on the CD4 D1 domain as a critical

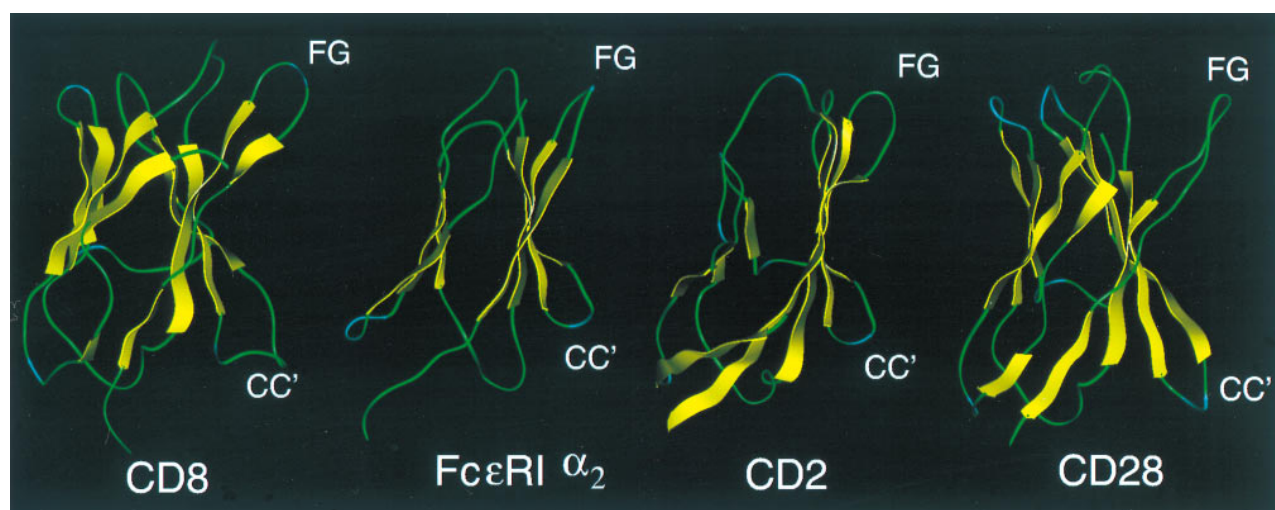


FIG. 6. Surface-binding pockets consisting of FG and CC' loops observed in: CD8 α , which mediates dimerization (35); Fc ϵ RI α_2 , which is the domain of IgE high-affinity receptor that binds IgE (36); CD2, which binds LFA-3 (37); and CD28, which binds CD80/86 (38). These surface interaction sites show a similar feature to that of the CD4 protein as shown in Fig. 1. The structure of Fc ϵ RI α_2 was modeled based on the crystal structures of CD2 domain 2 (37) and CD4 domain 2 (12). The structure of CD28 was modeled by using the crystal structure of the V_H chain of HYHEL-5 Fab (39).

functional epitope, involved either directly or indirectly in stable CD4–MHC class II interaction and T-cell activation. A computer-based data base screening strategy has been employed to identify a diverse group of novel non-peptidic organic ligands of this CD4 surface pocket that specifically block CD4–MHC class II cell adhesion and exhibit significant immunosuppressive activity in animal models of autoimmune disease and transplant rejection. This computer screening approach should have general implications for studying many Ig-related molecules that use similar surface structural features for diverse intermolecular binding and biological functions. Finally, the results from this study have demonstrated that the structure-based, computer-assisted design of small non-peptidic inhibitors of large protein–protein interfaces may indeed be an achievable goal.

We thank Dr. Daniel Butcher for technical assistance in the application of the computational software and Simei Shan and Zhixian Lu for peptide synthesis. This work was supported by funding from the Translational Research Committee of the Kimmel Cancer Institute.

1. Janin, J. & Chothia, C. (1990) *J. Biol. Chem.* **265**, 16027–16030.
2. Davies, D. R., Padlan, E. A. & Sheriff, S. (1990) *Annu. Rev. Biochem.* **59**, 439–473.
3. Clackson, T. & Wells, J. A. (1995) *Science* **267**, 383–386.
4. Livnah, O., Stura, E. A., Johnson, D. L., Middleton, S. A., Mulcahy, L. S., Wrighton, N. C., Dower, W. J., Jolliffe, L. K. & Wilson, I. A. (1996) *Science* **273**, 464–471.
5. Williams, A. F. & Barclay, A. N. (1988) *Annu. Rev. Immunol.* **6**, 381–405.
6. White, R. A. H., Mason, D. W., Williams, A. F., Galfre, G. & Milstein, C. (1978) *J. Exp. Med.* **148**, 664–673.
7. Miceli, M. C. & Parnes, J. R. (1993) *Adv. Immunol.* **53**, 59–122.
8. Doyle, C. & Strominger, J. L. (1987) *Nature (London)* **356**, 626–629.
9. Konig, R., Huang, L.-Y. & Germain, R. N. (1992) *Nature (London)* **356**, 796–798.
10. Weber, S. & Karjalainen, K. (1993) *Int. Immunol.* **5**, 695–698.
11. Ryu, S. E., Kwong, P. D., Truneh, A., Porter, T. G., Arthos, J., Rosenberg, M., Dai, X., Xuong, N. H., Axel, R., Sweet, R. W. & Hendrickson, W. A. (1990) *Nature (London)* **348**, 419–426.
12. Wang, J., Yan, Y., Garrett, T. P. J., Liu, J., Rodgers, D. W., Garlick, R. L., Tarr, G. E., Husain, Y., Reinherz, E. L. & Harrison, S. C. (1990) *Nature (London)* **348**, 411–418.
13. Brown, J. H., Jardetzky, T. S., Gorga, J. C., Stern, L. J., Urban, R. G., Strominger, J. L. & Wiley, D. C. (1993) *Nature (London)* **364**, 33–39.
14. Clayton, L. K., Sieh, M., Pious, D. A. & Reinherz, E. L. (1989) *Nature (London)* **339**, 548–551.
15. Lamarre, D., Ashkenazi, A., Fleury, S., Smith, D. H., Sekaly, R. P. & Capon, D. J. (1989) *Science* **245**, 743–746.
16. Fleury, S., Lamarre, D., Meloche, S., Ryu, S.-E., Cantin, C., Hendrickson, W. A. & Sekaly, R. P. (1991) *Cell* **66**, 1037–1049.
17. Kuntz, I. D. (1992) *Science* **257**, 1078–1082.
18. Ring, C. S., Sun, E., McKerrow, J. H., Lee, G. K., Rosenthal, P. J., Kuntz, I. D. & Cohen, F. E. (1993) *Proc. Natl. Acad. Sci. USA* **90**, 3583–3587.
19. Meng, E. C., Shoichet, B. K. & Kuntz, I. D. (1992) *J. Comput. Chem.* **13**, 505–524.
20. Moebius, U., Clayton, L. K., Abraham, S., Diener, A., Yunis, J. J., Harrison, S. C. & Reinherz, E. L. (1992) *Proc. Natl. Acad. Sci. USA* **89**, 12008–12012.
21. MacRae, B. L., Nikcevich, K. M., Karpus, W. J., Hurst, S. D. & Miller, S. D. (1995) *J. Neuroimmunol.* **60**, 17–28.
22. Korngold, R., Feldman, A., Rorke, L. B., Lublin, F. D. & Doherty, P. C. (1986) *Immunogenetics* **24**, 309–315.
23. Bailey, D. W. & Usama, B. (1960) *Transplant. Bull.* **7**, 424–425.
24. Satoh, T., Li, S., Friedman, T. M., Wiaderekiewicz, R., Korngold, R. & Huang, Z. (1996) *Biochem. Biophys. Res. Commun.* **224**, 438–443.
25. Peters, K. P., Fauck, J. & Frommel, C. (1996) *J. Mol. Biol.* **256**, 201–213.
26. Lee, B. & Richards, F. M. (1971) *J. Mol. Biol.* **55**, 379–400.
27. Gilson, M. K., Sharp, K. A. & Honig, B. H. (1988) *J. Comput. Chem.* **9**, 327–335.
28. Langedijk, J. P. M., Puijk, W. C., van Hoorn, W. P. & Meloen, R. H. (1993) *J. Biol. Chem.* **268**, 16875–16878.
29. Jameson, B. A., McDonnell, J. M., Marini, J. C. & Korngold, R. (1994) *Nature (London)* **368**, 744–746.
30. Friedman, T. M., Reddy, A. P., Wassell, R. & Korngold, R. (1996) *J. Biol. Chem.* **271**, 22635–22640.
31. Zhang, X., Piatier-Tonneau, D., Auffray, C., Murali, R., Mahapatra, A., Zhang, F., Maier, C. C., Saragovi, H. & Greene, M. I. (1996) *Nature Biotechnology* **14**, 472–475.
32. Hafler, D. A., Ritz, J., Schlossman, S. F. & Weiner, H. L. (1988) *J. Immunol.* **141**, 131–138.
33. Hruby, V. J. (1993) *Biopolymers* **33**, 1073–1082.
34. Combs, A. P., Kapoor, T. M., Feng, S. B., Chen, J. K., Daudesnow, L. F. & Schreiber, S. L. (1996) *J. Am. Chem. Soc.* **118**, 287–288.
35. Leahy, D. J., Axel, R. & Hendrichson, W. A. (1992) *Cell* **68**, 1145–1162.
36. McDonnell, J. M., Beavil, A. J., Mackay, G. A., Jameson, B. A., Korngold, R., Gould, H. J. & Sutton, B. J. (1996) *Nat. Struct. Biol.* **3**, 419–426.
37. Jones, E. Y., Davis, S. J., Williams, A. F., Harlos, K. & Stuart, D. I. (1992) *Nature (London)* **360**, 232–239.
38. Linsley, P. S., Clark, E. A. & Ledbetter, J. A. (1990) *Proc. Natl. Acad. Sci. USA* **87**, 5031–5035.
39. Sheriff, S., Silverton, E. W., Padlan, E. A., Cohen, G. H., Smith-Gill, S. J., Finzell, B. C. & Davies, D. R. (1987) *Proc. Natl. Acad. Sci. USA* **84**, 8075–8079.
40. Lascombe, M. B., Alzari, P. M., Boulot, G., Saludjian, P., Tougard, P., Berek, C., Haba, S., Rosen, E. M., Nisonoff, A. & Poljak, R. J. (1989) *Proc. Natl. Acad. Sci. USA* **86**, 607–611.
41. Springer, T. A. (1990) *Nature (London)* **346**, 425–434.